



# HHS Public Access

Author manuscript

*Neurobiol Aging*. Author manuscript; available in PMC 2024 October 01.

Published in final edited form as:

*Neurobiol Aging*. 2023 October ; 130: 103–113. doi:10.1016/j.neurobiolaging.2023.06.014.

Corresponding Author: Andrew J. Saykin, asaykin@iupui.edu, Address: 355 W. 16<sup>th</sup> Street GH Suite 4100, Indianapolis, IN 46202.

**Publisher's Disclaimer:** This is a PDF file of an unedited manuscript that has been accepted for publication. As a service to our customers we are providing this early version of the manuscript. The manuscript will undergo copyediting, typesetting, and review of the resulting proof before it is published in its final form. Please note that during the production process errors may be discovered which could affect the content, and all legal disclaimers that apply to the journal pertain.

**Publisher's Disclaimer:** form, but we are providing this version to give early visibility of the article. Please note that, during the production process, errors may be discovered which could affect the content, and all legal disclaimers that apply to the journal pertain.

Declarations of Interest:

Dr. Apostolova receives support in the form of consulting fees from Biogen, Two Labs, IQVIA, NIH, Florida Department of Health, NIH Biobank, Eli Lilly, GE Healthcare, and Eisai; in the form of payment for lectures, etc. from AAN, MillerMed, AiSM, and Health and Hospitality; and in the form of travel and meeting support from Alzheimer's Association. She also participates on Data Safety Monitoring or Advisory boards for IQVIA, NIA R01 AG061111, UAB Nathan Shock Center, and New Mexico Exploratory ADRC; in leadership roles for Medical Science Council Alzheimer Association Greater IN Chapter, Alzheimer Association Science Program Committee, and FDA PCNS Advisory Committee; stock or stock options Cassava Neurosciences and Golden Seeds, and receipt of materials, etc. from AVID Pharmaceuticals, Life Molecular Imaging, and Roche Diagnostics.

Dr. Saykin has received support for consultation to Bayer Oncology (Scientific Advisory Board), Eisai (Scientific Advisory Board), Siemens Medical Solutions USA, Inc. (Dementia Advisory Board), and Springer-Nature Publishing (Editorial Office Support as Editor-in-Chief, Brain Imaging and Behavior).

Dr. Wang has received book royalties from American Psychiatric Publishing, Inc., and consultant fees for serving on a Data Safety Monitoring Board.

Dr. Clark receives royalties for two UpToDate articles on aphasia and has done paid consulting for Eli Lilly and Company on the topic of amyloid scans.

Dr. Brosch discloses the following: AbbVie [Progressive supranuclear palsy]; AbbVie [Alzheimer disease]; Avanir [Alzheimer disease]; Biogen [Alzheimer disease]; Biogen [Prodromal or mild Alzheimer disease]; Dominantly Inherited Alzheimer Network [Alzheimer disease]; Eisai [Early Alzheimer disease]; Eisai [Dementia with Lewy bodies]; Eli Lilly [Alzheimer disease]; Eli Lilly [Parkinson disease dementia]; Genentech [Alzheimer disease]; Novartis [Alzheimer disease]; Roche [Alzheimer disease]; Suven [Alzheimer disease].

All other authors report no disclosures.

CRedit authorship contribution statement

Cecily G. Swinford: conceptualization, methodology, formal analysis, writing-original draft, writing-review and editing, visualization  
Shannon L. Risacher: conceptualization, methodology, software, validation, data curation, writing- review and editing, supervision, funding acquisition

Aaron Vosmeier: investigation

Rachael Deardorff: software, validation, data curation, writing-review & editing

Evgeny J. Chumin: software, validation, data curation, writing-review & editing

Mario Dzemić: software, validation, data curation, writing-review & editing

Yu-Chien Wu: conceptualization, methodology, writing-review & editing, supervision

Sujuan Gao: conceptualization, methodology, writing-review & editing, supervision

Brenna C. McDonald: writing-review & editing, investigation

Karmen K. Yoder: writing-review & editing, investigation

Frederick W. Unverzagt: investigation

Sophia Wang: investigation, writing-review & editing

Martin R. Farlow: investigation, writing-review & editing

Jared R. Brosch: investigation, writing-review & editing

David G. Clark: investigation, writing-review & editing

Liana G. Apostolova: conceptualization, methodology, writing-review & editing, supervision, investigation

Justin Sims: investigation, writing-review & editing

Danny J. Wang: methodology, software, writing-review and editing

Andrew J. Saykin: conceptualization, methodology, resources, writing-review and editing, supervision, project administration, funding acquisition

Verification

The authors verify that the manuscript "Amyloid and Tau Pathology are Associated with Cerebral Blood Flow in a Mixed Sample of Nondemented Older Adults with and without Vascular Risk Factors for Alzheimer's Disease" has not been published previously and is not under consideration for publication elsewhere.

## Amyloid and Tau Pathology are Associated with Cerebral Blood Flow in a Mixed Sample of Nondemented Older Adults with and without Vascular Risk Factors for Alzheimer's Disease

Cecily G. Swinford<sup>a,b</sup>, Shannon L. Risacher<sup>a,b</sup>, Aaron Vosmeier<sup>a,b</sup>, Rachael Deardorff<sup>a,b</sup>, Evgeny J. Chumin<sup>b,e,f</sup>, Mario Dzemic<sup>b,d</sup>, Yu-Chien Wu<sup>a,b</sup>, Sujuan Gao<sup>b,g</sup>, Brenna C. McDonald<sup>a,b,d</sup>, Karmen K. Yoder<sup>a,b</sup>, Frederick W. Unverzagt<sup>b,h</sup>, Sophia Wang<sup>b,h</sup>, Martin R. Farlow<sup>b,d</sup>, Jared R. Brosch<sup>b,d</sup>, David G. Clark<sup>b,d</sup>, Liana G. Apostolova<sup>a,b,d,e</sup>, Justin Sims<sup>a</sup>, Danny J. Wang<sup>c</sup>, Andrew J. Saykin<sup>a,b,d,e</sup>

<sup>a</sup>)Department of Radiology and Imaging Sciences, Indiana University School of Medicine, 355 W. 16<sup>th</sup> Street, Goodman Hall, Suite 4100, Indianapolis, IN 46202

<sup>b</sup>)Indiana Alzheimer's Disease Research Center, 355 W. 16<sup>th</sup> Street, Goodman Hall, Suite 4100, Indianapolis, IN 46202

<sup>c</sup>)Stevens Neuroimaging and Informatics Institute, Keck School of Medicine of University of Southern California, SHN 2025 Zonal Ave. Los Angeles, CA 90033

<sup>d</sup>)Department of Neurology, Indiana University School of Medicine, 355 W. 16<sup>th</sup> Street Goodman Hall Suite 4700, Indianapolis, IN 46202

<sup>e</sup>)Indiana University Network Science Institute, 1015 E. 11<sup>th</sup> Street, Bloomington, IN 47408

<sup>f</sup>)Department of Psychological and Brain Sciences, Indiana University, 1101 E. 10<sup>th</sup> Street, Bloomington, IN 47405

<sup>g</sup>)Department of Biostatistics and Health Data Sciences, Indiana University School of Medicine, 410 W. 10<sup>th</sup> Street HITS 3000, Indianapolis, IN 46202

<sup>h</sup>)Department of Psychiatry, Indiana University School of Medicine, 355 W. 16<sup>th</sup> Street Goodman Hall, Indianapolis, IN 46202

### Abstract

Identification of biomarkers for early stages of Alzheimer's disease (AD) is an imperative step in developing effective treatments. Cerebral blood flow (CBF) is a potential early biomarker for AD; generally, older adults with AD have decreased CBF compared to normally aging peers. CBF deviates as the disease process and symptoms progress. However, further characterization of the relationships between CBF and AD risk factors and pathologies is still needed. We assessed the relationships between CBF quantified by arterial spin labeled MRI, hypertension, *APOE*  $\epsilon 4$ , and tau and amyloid PET in 77 older adults: cognitively normal, subjective cognitive decline, and mild cognitive impairment. Tau and amyloid aggregation were related to altered CBF, and some of these relationships were dependent on hypertension or *APOE*  $\epsilon 4$  status. Our findings suggest a complex relationship between risk factors, AD pathologies, and CBF that warrants future studies of CBF as a potential early biomarker for AD.

## Keywords

tau PET; amyloid PET; cerebral blood flow; arterial spin labeled MRI; biomarkers; mild cognitive impairment

---

## 1. Introduction

Over 6 million older adults in the U.S. have Alzheimer's disease (AD), and this number is projected to double over the next thirty years (Alzheimer's Disease Facts and Figures, 2021). The results of multiple studies and clinical trials suggest that an effective treatment for AD may need to be preventative (Jessen et al., 2014; Crous-Bou et al., 2017). Excluding at least one promising exception (van Dyck et al., 2023), treatments that target amyloid beta ( $A\beta$ ) and/or tau pathology have generally been unable to restore cognitive function after cognitive decline has occurred (Lu et al., 2020; Congdon and Sigurdsson, 2018). Preventative treatment will require reliable biomarkers for the preclinical stages of AD so that individuals most at risk can be accurately identified. One potential early biomarker that warrants further characterization is quantitative cerebral blood flow (CBF).

CBF is known to be decreased in individuals with AD compared to healthy individuals of the same age (Alsop et al., 2000; Swinford et al., 2022; Zhang et al., 2021), independently of brain atrophy (Binnewijzend et al., 2013). Additionally, vascular risk factors including hypertension, diabetes mellitus, and obesity are risk factors for AD (Gorelick, 2004), and they have been shown to have an effect on CBF (Bangen et al., 2014). Chronic hypertension, in particular, has been shown to cause cerebral microvascular damage, which both worsens and is worsened by  $A\beta$  aggregation (Iadecola and Gottesman, 2019). It has been suggested that altered CBF may occur very early in the course of AD, before cognitive decline and potentially even prior to  $A\beta$  and tau aggregation (Iadecola, 2004).

However, the spatial and temporal patterns of CBF alteration over the course of AD have not been fully characterized. It has been shown that CBF increases in some brain regions, especially in preclinical and prodromal AD, known as subjective cognitive decline (SCD) and mild cognitive impairment (MCI; Beishon et al., 2017; Dai et al., 2009). However, most individuals have decreased CBF by the time they meet criteria for AD (Swinford et al., 2022; Wierenga et al., 2014). Increased CBF in SCD and early MCI may compensate to maintain a level of cognitive functioning despite pathologies such as  $A\beta$  and/or tau aggregation for a limited time. It is important to elucidate the spatial and temporal relationships between altered CBF, other AD-related pathologies, and vascular risk factors. Here, in older adults who are cognitively normal (CN), SCD, and MCI, we assessed the relationships between CBF and global cortical  $A\beta$  and medial temporal lobe (MTL) tau pathology using arterial spin labeled (ASL) magnetic resonance imaging (MRI) and positron emission tomography (PET). We also assessed the interaction effects of hypertension and *APOE*  $\epsilon 4$  positivity on these relationships. We hypothesized that  $A\beta$  and tau pathologies would negatively correlate with CBF overall, although localized regions of positive correlation would be present as well, given the early stage of disease in this sample. We also hypothesized that individuals with hypertension or at least one *APOE*  $\epsilon 4$

allele would be less likely to have a compensatory positive correlation between CBF and AD-related pathologies.

## 2. Methods

### 2.1 Participants

This study included 77 participants (30 CN, 24 SCD, 23 MCI) from the Indiana Alzheimer's Disease Research Center who were at least sixty years of age. All participants completed T1-weighted structural and pseudocontinuous arterial spin labeled (pCASL) MRI scans, A $\beta$  PET scan with either [<sup>18</sup>F]florbetapir or [<sup>18</sup>F]florbetaben, and tau PET scan with [<sup>18</sup>F]flortaucipir. All participants also had a clinical assessment including administration of the objective neuropsychological test battery Uniform Data Set version 3 (UDS 3.0; Besser et al., 2018) and *APOE* genotyping. Diagnoses were determined by clinician consensus. SCD was defined as a score of 20 or more on the first 12 items of the 20-item Cognitive Change Index (CCI-20; Saykin et al., 2006), reflecting increased subjective memory concerns, with or without increased levels of informant-based concerns (Jessen et al., 2014), and the absence of a measurable cognitive deficit on the UDS 3.0. Using standard criteria, an individual was diagnosed with MCI if the participant and/or an informant had a significant complaint about their cognition, and the participant scored 1.5 standard deviations or more below age-, education-, and sex-adjusted normative data on objective tests of cognitive functioning in the UDS 3.0 either in memory or another cognitive domain. Additionally, individuals diagnosed with MCI, by definition, do not show a significant decline in daily functioning.

Hypertension was defined as a previous diagnosis of hypertension via self-report near the time of imaging. It has been shown that midlife hypertension, rather than hypertension later in life, confers the greatest risk for AD later in life (Lennon et al., 2021; Whitmer et al., 2005). Some hypertensive individuals were taking antihypertensive medication at the time of the study. A vascular risk score was calculated for each participant. We used a simple point-based score informed by the Framingham Heart Study vascular risk score (Wilson et al., 1998). Each participant received one vascular risk point for each of the following conditions: self-reported diabetes and/or use of diabetes medication, self-reported hypercholesterolemia and/or use of medication for high cholesterol, obesity as defined by BMI greater than 30, and blood pressure that meets criteria for hypertension (systolic blood pressure equal to or greater than 130 and/or diastolic blood pressure equal to or greater than 80) taken from the appointment closest to the ASL MRI scan. Vascular risk scores ranged from 0 to 4 points. All procedures were approved by the Indiana University School of Medicine Institutional Review Board. Informed consent was obtained according to the Declaration of Helsinki and the Belmont Report.

### 2.2 pCASL and T1-weighted MRI

All MRI scans were acquired on the same Siemens 3T Prisma scanner with a 64-channel head/neck radiofrequency coil. After an initial T1-weighted structural scan (sagittal 3D MPRAGE) each participant completed a 3D pseudo-continuous ASL (pCASL) MRI scan.

Processing steps were performed using Statistical Parametric Mapping 12 (SPM12; Wellcome Department of Cognitive Neuroscience, London, UK) and Matlab R2022a as previously described (Butcher et al., 2021; Wang et al., 2003). To calculate CBF from pCASL images, pairs of pCASL images were subtracted and then averaged to obtain a mean perfusion image. A standard single-compartment perfusion model (Alsop et al., 2015) was used to calculate mean CBF maps from the mean perfusion images (<http://cfn.upenn.edu/perfusion/software.htm>). Using each individual's gray matter tissue map from the structural MRI, an individualized gray matter mask was applied to each mean CBF map, and the cerebellum was excluded in order to remove individual variability in this region, which is common with pCASL imaging. CBF was extracted from the resulting masked CBF map from frontal, parietal, temporal, and occipital lobes and limbic regions of interest (ROIs) using Automated Anatomical Labeling (AAL) version 1 and the MarsBaR toolbox (Brett et al., 2002).

### 2.3 A $\beta$ PET

Each participant underwent either a [ $^{18}\text{F}$ ]florbetapir (AmyVid; Eli Lilly and Co.) or a [ $^{18}\text{F}$ ]florbetaben (Neuraceq; Life Molecular Imaging, formerly Piramal Imaging) scan. A $\beta$  PET data was recorded in four 5-minute frames and reconstructed using standard Siemens scanner parameters as defined in the Alzheimer's Disease Neuroimaging Initiative (ADNI) 2 protocol (Jagust et al., 2015; <https://adni.loni.usc.edu/methods/pet-analysis-method/pet-analysis/>) and in the Supplemental file. Each 5-minute frame was spatially aligned to the participant's T1-weighted structural MRI using SPM12. The spatially aligned PET images were averaged to create a single image from the total acquisition time period for each individual, and standardized uptake value ratio (SUVR) images were generated by intensity normalizing with the average radioactivity from a whole cerebellar region of interest from the Centiloid project (<http://www.gaain.org/Centiloid-project/>). For this study, we used the global cortical A $\beta$  measure calculated in Centiloid units, a unified metric that allowed us to directly compare data from both scan types. The global cortical ROI was determined by the Centiloid project and is the ROI for which use of Centiloid units is intended. Both types of scans were processed with the Centiloid algorithm at a voxel-wise level as defined by the Centiloid project (Risacher et al., 2021). Global cortical Centiloid data were then extracted from both scan types using the MarsBaR toolbox (Brett et al., 2002).

### 2.4 Tau PET

All participants underwent a [ $^{18}\text{F}$ ]flortaucipir PET scan. Individuals were imaged on the same Siemens Biograph mCT PET/CT scanner for 30 minutes; data were binned into six 5-minute frames, and scans were reconstructed using a standard scanner software program (Siemens, Knoxville, TN) according to the ADNI2 protocol (Jagust et al., 2015; <https://adni.loni.usc.edu/methods/pet-analysis-method/pet-analysis/>) as further described in the Supplemental file. The 5-minute frames were spatially aligned to each participant's T1 image and normalized to MNI space, averaged to create a single image, intensity normalized by the cerebellar crus (Schwarz et al., 2016) to create SUVR images, and smoothed, all using SPM12. For this study, we extracted the MTL SUVR. This region was chosen because it is the main location of tau aggregation in early stages of AD, including SCD and MCI, so it was considered the region most likely to correlate with disease severity in

our sample. The constituent ROIs were generated from FreeSurfer 6.0 (Fischl and Dale, 2000; <http://surfer.nmr.mgh.harvard.edu/>), and the bilateral mean MTL (average of fusiform gyri, parahippocampal gyri, and entorhinal cortex) SUVR values were extracted for each participant using MarsBaR.

## 2.5 Statistical Analyses

The demographic and clinical variables, as well as global CBF, total gray matter volume, and  $A\beta$  and tau PET measures were compared between diagnostic groups using one-way ANOVA for continuous variables and chi-square test for categorical variables. Total gray matter volume was included as a covariate in subsequent analyses to confirm that decreased CBF is indicative of hypoperfusion rather than a decreased need for CBF in line with decreased brain tissue. Stepwise multiple regression models (entry  $p=0.10$ , removal  $p=0.20$ ) with dependent variable regional CBF and independent variables, age, sex, diagnostic group, total gray matter volume (from T1-weighted image gray matter estimates by SPM12 tissue volume utility), self-reported hypertension status, *APOE*  $\epsilon 4$  status, vascular risk score, and use of antihypertensive medication were used to determine demographic and clinical variables that correlated with CBF in this sample. Additionally,  $A\beta$  and tau PET metrics were treated as the dependent variables in multiple regression models with age, sex, diagnostic group, total gray matter volume, self-reported hypertension status, *APOE*  $\epsilon 4$  status, vascular risk score, and use of antihypertensive medication as independent variables to assess correlations between  $A\beta$  and tau PET and demographic and clinical variables. Partial Pearson correlations assessed the relationships between regional CBF and  $A\beta$  or tau PET metrics, with age, sex, diagnostic group, total gray matter volume as covariates. Self-reported hypertension status, *APOE*  $\epsilon 4$  status, vascular risk score, and use of antihypertensive medication were added as covariates. Voxel-wise analyses using multiple regression with CBF maps as the dependent variable,  $A\beta$  or tau PET metric as the independent variable, and age, sex, diagnostic group and total gray matter volume as covariates were used to explore associations that may not have been detectable when using the lobar regions of interest. Voxel-wise analyses were also used to explore the effects of the interactions between  $A\beta$  or tau PET metrics and self-reported hypertension or *APOE*  $\epsilon 4$  status on CBF with  $A\beta$  or tau PET metric, self-reported hypertension or *APOE*  $\epsilon 4$  status, age, sex, diagnostic group and total gray matter volume as covariates. CBF was extracted from significant clusters and modeled as the dependent variable in linear regression to visualize interactions. Results are listed at threshold  $p < 0.001$  and cluster size ( $k > 50$  voxels (uncorrected) for clusters with peak voxels within labeled gray matter regions. All voxel-wise analyses were completed using SPM12. Other statistical analyses and all graphs were created in IBM SPSS 25. Supplementary Figure 1 is a schematic that lists the analyses, with their variables and covariates, used in this manuscript.

## 3. Results

### 3.1 Demographics

Demographics and clinical variables are given in Table 1. The MCI group had a greater global cortical Centiloid value than the CN (Bonferroni  $T=3.54$ ,  $p=0.002$ ) and SCD (Bonferroni  $T=3.08$ ,  $p=0.009$ ) groups ( $F(2, 76) = 7.24$ ,  $p=0.001$ ). Diagnostic groups also

differed by prevalence of self-reported hypertension ( $\chi^2(2)=11.09$ ,  $p=0.004$ ) but did not differ by blood pressure taken at the time of scan ( $p>0.05$ ). The SCD group had the highest prevalence of self-reported hypertension, followed by MCI, and then by CN. There is a trend level difference in prevalence of antihypertensive medication use ( $\chi^2(2)=5.59$ ,  $p=0.061$ ). Prevalence was highest in the SCD group, followed by MCI and then CN. Neither global CBF nor the vascular risk score differed by diagnostic group ( $p>0.05$ ).

### 3.2 CBF vs. Demographic and Clinical Variables

Age and self-reported hypertension were negatively correlated with CBF in all lobes, and female sex was positively correlated with CBF in limbic and occipital lobes (Table 2). When this analysis was repeated with stratification by diagnostic group, age was negatively correlated with CBF in the CN group, self-reported hypertension was negatively correlated with CBF in the frontal lobe in the MCI group, and female sex was positively correlated with CBF in the MCI group (Supplementary Tables 1 and 2). Voxel-wise regressions were used to spatially model these relationships, revealing more widespread negative correlations between self-reported hypertension and CBF in the MCI group when the vascular risk score and use of antihypertensive medication were included as covariates (Figures 1 and 2, Supplementary Figures 2 and 3, Supplementary Tables 3–7).

### 3.3 Tau and A $\beta$ PET vs. Demographic and Clinical Variables

The global cortical Centiloid value was positively associated with *APOE*  $\epsilon 4$  status ( $\beta=0.388$ ,  $t=3.992$ ,  $p<0.001$ ) and MCI ( $\beta=0.356$ ,  $t=3.657$ ,  $p<0.001$ ). None of the independent variables were entered into the model for MTL tau SUVR ( $p>0.05$ ). When the analyses were repeated with stratification by diagnostic group, the global cortical Centiloid value was positively associated with *APOE*  $\epsilon 4$  status in the CN group ( $\beta=0.455$ ,  $t=2.703$ ,  $p=0.012$ ) and in the MCI group ( $\beta=0.476$ ,  $t=2.483$ ,  $p=0.022$ ). The MTL tau SUVR was positively associated with age in the SCD group ( $\beta=0.517$ ,  $t=2.836$ ,  $p=0.010$ ) and negatively associated with age ( $\beta=-0.369$ ,  $t=-2.103$ ,  $p=0.048$ ) and self-reported hypertension ( $\beta=-0.545$ ,  $t=-3.104$ ,  $p=0.006$ ) in the MCI group.

### 3.4 Tau PET vs. Regional CBF

Partial correlations between lobar CBF and MTL tau SUVR were not significant regardless of whether self-reported hypertension, *APOE*  $\epsilon 4$  status, vascular risk score, and use of antihypertensive medication were included as covariates ( $p>0.05$ ). There was a trend level negative correlation between MTL tau SUVR and parietal lobe CBF in the SCD group ( $r=-0.416$ ,  $p=0.061$ ) with age, sex, and total gray matter volume as covariates. Using voxel-wise regression models with age, sex, diagnostic group and total gray matter volume as covariates, MTL tau SUVR was negatively correlated with CBF in the left parahippocampal gyrus in the full sample ( $p=0.001$ ,  $k=50$ ; Figure 3, Supplementary Table 8). MTL tau SUVR was negatively correlated with CBF in the left primary sensory, right primary motor, and right visual motor regions in the SCD group ( $p=0.001$ ,  $k=50$ ; Figure 3, Supplementary Table 9).

There were positive correlations between the MTL tau SUVR and self-reported hypertension status interaction variable and CBF in several brain regions in the SCD group ( $p=0.001$ ,

$k = 50$ ; Supplementary Table 10). There were negative correlations between the MTL tau SUVR and *APOE*  $\epsilon 4$  status interaction variable and spatially widespread CBF in the SCD group ( $p = 0.001$ ,  $k = 50$ ; Figure 4, Supplementary Table 11, Supplementary Figure 4) and a positive correlation between the MTL tau SUVR and *APOE*  $\epsilon 4$  status interaction variable and CBF in the right fusiform in the MCI group ( $p = 0.001$ ,  $k = 50$ ; Supplementary Table 12).

### 3.5 A $\beta$ PET vs. Regional CBF

Partial correlations between lobar CBF and global cortical Centiloid were not significant regardless of whether self-reported hypertension, *APOE*  $\epsilon 4$  status, vascular risk score, and use of antihypertensive medication were included as covariates ( $p > 0.05$ ). Using voxel-wise regression models with age, sex, diagnostic group and total gray matter volume as covariates, there were no statistically significant correlations between CBF and global cortical Centiloid at the  $p = 0.001$ ,  $k = 50$  level. However, there was a positive correlation between global cortical Centiloid and CBF in the right visual association region in the CN group ( $p = 0.001$ ,  $k = 50$ ; Figure 5, Supplementary Table 13) and a negative correlation between global cortical Centiloid and CBF in the right fusiform in the MCI group ( $p = 0.001$ ,  $k = 50$ ; Figure 5, Supplementary Table 14). There was a positive correlation between the global cortical Centiloid and self-reported hypertension interaction variable and CBF in the left visual motor region in the whole sample ( $p = 0.001$ ,  $k = 50$ ; Figure 6, Supplementary Table 15, Supplementary Figure 5). There was a positive correlation between the global cortical Centiloid and self-reported hypertension status interaction variable and CBF in the right hippocampus in the SCD group ( $p = 0.001$ ,  $k = 50$ ; Supplementary Table 16) and a positive correlation between the global cortical Centiloid and self-reported hypertension status interaction variable and CBF in the left frontal eye fields in the MCI group ( $p = 0.001$ ,  $k = 50$ ; Supplementary Table 17).

## 4. Discussion

Here, we assessed the relationships between CBF, AD pathologies imaged with PET (global cortical Centiloid and MTL tau SUVR), and AD risk factors (including self-reported hypertension and *APOE*  $\epsilon 4$  status) in a sample of CN, SCD, and MCI older adults. Both self-reported hypertension and MTL tau SUVR were negatively associated with CBF among and within diagnostic groups in exploratory voxel-wise analyses. Although altered, some negative associations between self-reported hypertension and CBF remained when vascular risk score and use of antihypertensive medication were taken into account. Global cortical Centiloid was positively associated with CBF in the CN and negatively associated with CBF in the MCI group in voxel-wise analyses. Finally, there were effects of AD pathology and vascular risk factor interaction variables on CBF in voxel-wise analyses. These include a negative effect of the MTL tau SUVR and *APOE*  $\epsilon 4$  status interaction variable on CBF in the SCD group and a positive effect of the global cortical centiloid and self-reported hypertension status interaction variable on CBF in the full sample. While these findings generally follow our hypotheses, they also suggest that the relationships among these factors are complex and dynamic.

Previous studies, briefly described below, concerning the relationship between tau and CBF have reported negative correlations that track both spatially and temporally with disease severity and brain dysfunction (Ashford et al., 2000; Gomez-Isla et al., 1997). Animal models of hypoperfusion develop increased tau pathology (Raz et al., 2019; Zhang et al., 2010), and animal models of tau pathology develop hypoperfusion (Bennett et al., 2018; Jaworski et al., 2011; Lourenco et al., 2017; Park et al., 2020). In human studies in preclinical and/or clinical AD, there have been findings of negative correlations between tau pathology and CBF in temporal, parietal, and occipital lobes, and entorhinal cortex (Albrecht et al., 2020; Rubinski et al., 2021; Visser et al., 2020). Studies in CN individuals report a mix of results; Hays et al. (2020) reported a negative correlation between CSF tau and CBF in the anterior cingulate cortex, while Stomrud et al. (2012) reported a positive correlation between tau and CBF in the frontotemporal border zone and a negative correlation between tau and CBF in the medial frontal lobe. Another study reported that asymptomatic individuals with the same amount of tau pathology as individuals with MCI had increased CBF in the MTL and thalamus over time (Codispoti et al., 2012). Although there are fewer studies focused on the relationship between tau pathology and CBF compared to A $\beta$  pathology, it appears that a similar overall pattern of findings is emerging, with some positive correlations in early disease stages and negative correlations in later stages.

Negative correlations between A $\beta$  pathology and CBF have been heavily documented. For example, several animal models of chronic hypoperfusion have been shown to develop A $\beta$  pathology (Chan et al., 2018; de la Torre et al., 2003; Faraco et al., 2016; Khan et al., 2015; Liang et al., 2015), and animal models of A $\beta$  pathology, likewise, develop decreased CBF (Klohs et al., 2014; Niwa et al., 2001). Studies involving participants with preclinical and/or clinical AD have shown negative correlations between A $\beta$  pathology and CBF in entorhinal regions, the precuneus, and throughout the cortex (Mattsson et al., 2014; Rodell et al., 2016). Chen et al. (2015), on the other hand, reported a positive correlation between A $\beta$  and CBF in the anterior cingulate gyrus in a mixed sample including AD patients. Michels et al. (2016) and Tosun et al. (2016) both reported negative correlations between A $\beta$  PET and CBF in regions including frontal, temporal, parietal, and occipital lobes, cingulate cortex, and cerebellum in disease stages prior to AD. In a sample of A $\beta$ -positive CN individuals, A $\beta$  was positively correlated with CBF in frontal and temporal lobes, insula, dorsal striatum, hippocampus, and amygdala (Fazlollahi et al., 2020).

Interacting relationships between vascular risk factors and AD pathologies and symptoms have been previously studied. Specifically, two papers (Wang et al., 2019; Zlatar et al., 2016) reported a positive correlation between CBF and cognition in *APOE*  $\epsilon$ 4-negative CN individuals and a negative correlation between CBF and cognition in *APOE*  $\epsilon$ 4-positive CN individuals. Hays et al. (2020) found a negative relationship between tau in the cerebrospinal fluid and CBF in the anterior cingulate in *APOE*  $\epsilon$ 4-positive but not *APOE*  $\epsilon$ 4-negative individuals. *APOE*  $\epsilon$ 4 is associated with increased A $\beta$  aggregation, most likely by reducing the clearance of A $\beta$  from the brain and increasing its production (Castellano et al., 2011; Donahue and Johanson, 2008; Mahley et al., 2006; Wahrle et al., 2007). It has also been reported that *APOE*  $\epsilon$ 4 carriers have increased levels of tau in the MTL (Jack et al., 2020; Ossenkoppele et al., 2016).

Our findings are generally in line with current literature. As we expected, both self-reported hypertension and MTL tau SUVR are negatively correlated with CBF in this sample. Self-reported hypertension appeared to be particularly associated with decreased CBF in the MCI group, while MTL tau SUVR appeared to be particularly associated with decreased CBF in the SCD group. In the SCD group, regions of CBF were negatively correlated with MTL tau SUVR in *APOE*  $\epsilon$ 4 positive individuals and positively correlated with MTL tau SUVR in *APOE*  $\epsilon$ 4 negative individuals. It is possible that individuals with *APOE*  $\epsilon$ 4 are more susceptible to hypoperfusion related to tau pathology in early disease stages. Global cortical Centiloid was positively correlated with CBF in the CN group but negatively correlated with CBF in the MCI group. This follows the general trend of compensatory mechanisms in early disease stages followed by loss of compensation and deterioration of brain function as the disease progresses. Our finding of a positive correlation between global cortical Centiloid and CBF in individuals with self-reported hypertension but a negative correlation between global cortical Centiloid and CBF in individuals without self-reported hypertension across all diagnostic groups suggests that A $\beta$  aggregation and hypertension may not have strictly additive effects on brain function. This interaction was not in the direction that we expected, but there is not yet a standard time course for compensation versus failure of compensation, and it likely differs for each individual based on comorbidities, cardiovascular health, lifestyle choices like diet and exercise, and demographic, genetic, and environmental variables. Our findings suggest that the combined effects of vascular risk factors, AD pathology, and AD-specific risk factors on CBF warrant further research with large and diverse patient samples.

This study was limited by its modest sample size. Some regions of association between voxel-wise CBF and PET biomarkers did not reach statistical significance, and a larger sample size could have led to more statistically significant results suggesting a clearer picture of correlative patterns. Future studies should use larger sample sizes of individuals with preclinical AD so that statistical power is adequate to elucidate the complex relationships between CBF, A $\beta$ , tau, and other AD-related pathologies. Our sample was also homogenous in terms of ethnoracial and educational backgrounds, making our findings most applicable to a subset of the population of older adults at risk for AD. It will be important to utilize diverse samples in future studies. Additionally, our use of MTL tau SUVR, while it is the region most likely involved in early stage tau aggregation did not allow us to take atypical patterns of tau aggregation into account in this study. Finally, we defined hypertension by self-report rather than by a threshold blood pressure at the time of scanning, and some hypertensive individuals were taking antihypertensive medications. We included blood pressure as part of our vascular risk score and included this score and use of antihypertensives in a number of our models, but future studies with a narrower definition of hypertension may be beneficial.

#### 4.1 Conclusions

Our findings suggest complex spatial and temporal relationships among genetic and vascular risk factors, AD pathologies, and CBF in older adults at risk for AD. Specifically, the association between CBF and global cortical Centiloid differed according to diagnostic group (positive associations in CN and negative associations in MCI). Additionally, vascular

risk factors self-reported hypertension and *APOE*  $\epsilon$ 4 status influenced the relationships of global cortical Centiloid and MTL tau SUVR to CBF. These findings suggest that multiple interacting variables must be taken into account in order to characterize ASL MRI CBF as an early biomarker for AD and could help to inform future research in this area. This endeavor is likely to be greatly worthwhile; a reliable early biomarker for AD would allow us to identify those at risk for AD so that they can enter clinical trials and/or receive treatment in the future. An early biomarker could also allow us to track disease progression in both treated and untreated individuals, and perhaps to help elucidate the complex mechanisms that initiate AD and drive its progression. Future studies assessing the potential of CBF as an early biomarker for AD are warranted.

## Supplementary Material

Refer to Web version on PubMed Central for supplementary material.

## Acknowledgements:

John D. West, MSEng, Indiana University School of Medicine, played a primary role in optimizing and automating the pCASL processing pipeline, and the authors are grateful for his contributions to this research which we dedicate to his memory. We are grateful to the research participants and their families without whose generosity and commitment this study would not have been possible.

## Funding:

This study was funded in part by the following grants from the National Institute on Aging: K01 AG049050, R01 AG061788, P30 AG010133, P30 AG072976, R01 AG019771, R01 AG057739, U01 AG024904, R01 AG068193, T32 AG071444, U01 AG068057, and U01 AG072177 and the National Library of Medicine: R01 LM013463. In kind support for tau PET tracer precursor was provided by Avid Radiopharmaceuticals, a subsidiary of Eli Lilly and Company.

## Abbreviations:

|                            |   |
|----------------------------|---|
| <b>A<math>\beta</math></b> | amyloid beta                                |
| <b>AAL</b>                 | Automated Anatomical Labeling               |
| <b>AD</b>                  | Alzheimer's disease                         |
| <b>ADNI</b>                | Alzheimer's Disease Neuroimaging Initiative |
| <b>APOE</b>                | apolipoprotein E                            |
| <b>ANCOVA</b>              | analysis of covariance                      |
| <b>ANOVA</b>               | analysis of variance                        |
| <b>ASL</b>                 | arterial spin labeled                       |
| <b>CBF</b>                 | cerebral blood flow                         |
| <b>CCI</b>                 | Cognitive Change Index                      |
| <b>CN</b>                  | cognitively normal                          |
| <b>CSF</b>                 | cerebrospinal fluid                         |

|              |   |
|--------------|---|
| <b>FWE</b>   | Family-Wise Error                           |
| <b>FWHM</b>  | full width at half maximum                  |
| <b>MCI</b>   | mild cognitive impairment                   |
| <b>MNI</b>   | Montreal Neurological Institute             |
| <b>MRI</b>   | magnetic resonance imaging                  |
| <b>MTL</b>   | medial temporal lobe                        |
| <b>pCASL</b> | psuedocontinuous arterial spin labeled      |
| <b>PET</b>   | positron emission tomography                |
| <b>PIB</b>   | Pittsburgh compound B                       |
| <b>ROI</b>   | region of interest                          |
| <b>SCD</b>   | subjective cognitive decline                |
| <b>SPM</b>   | Statistical Parametric Mapping              |
| <b>SPSS</b>  | Statistical Package for the Social Sciences |
| <b>SUVR</b>  | standardized uptake value ratio             |

## References

- 2021 Alzheimer's disease facts and figures. *Alzheimers Dement* 2021;17(3):327–406. Epub 2021/03/24. doi: 10.1002/alz.12328. [PubMed: 33756057]
- Albrecht D, Isenberg AL, Stradford J, Monreal T, Sagare A, Pachicano M, Sweeney M, Toga A, Zlokovic B, Chui H, Joe E, Schneider L, Conti P, Jann K, Pa J. Associations between Vascular Function and Tau PET Are Associated with Global Cognition and Amyloid. *J Neurosci* 2020;40(44):8573–86. Epub 2020/10/14. doi: 10.1523/JNEUROSCI.1230-20.2020. [PubMed: 33046556]
- Alsop DC, Detre JA, Golay X, Gunther M, Hendrikse J, Hernandez-Garcia L, Lu H, MacIntosh BJ, Parkes LM, Smits M, van Osch MJ, Wang DJ, Wong EC, Zaharchuk G. Recommended implementation of arterial spin-labeled perfusion MRI for clinical applications: A consensus of the ISMRM perfusion study group and the European consortium for ASL in dementia. *Magn Reson Med* 2015;73(1):102–16. Epub 2014/04/10. doi: 10.1002/mrm.25197. [PubMed: 24715426]
- Alsop DC, Detre JA, Grossman M. Assessment of cerebral blood flow in Alzheimer's disease by spin-labeled magnetic resonance imaging. *Ann Neurol* 2000;47(1):93–100. Epub 2000/01/13. [PubMed: 10632106]
- Ashford JW, Shih WJ, Coupal J, Shetty R, Schneider A, Cool C, Aleem A, Kiefer VH, Mendiondo MS, Schmitt FA. Single SPECT measures of cerebral cortical perfusion reflect time-index estimation of dementia severity in Alzheimer's disease. *J Nucl Med* 2000;41(1):57–64. Epub 2000/01/27. [PubMed: 10647605]
- Bangen KJ, Nation DA, Clark LR, Harmell AL, Wierenga CE, Dev SI, Delano-Wood L, Zlatar ZZ, Salmon DP, Liu TT, Bondi MW. Interactive effects of vascular risk burden and advanced age on cerebral blood flow. *Front Aging Neurosci* 2014;6:159. Epub 2014/07/30. doi: 10.3389/fnagi.2014.00159. [PubMed: 25071567]
- Beishon L, Haunton VJ, Panerai RB, Robinson TG. Cerebral Hemodynamics in Mild Cognitive Impairment: A Systematic Review. *J Alzheimers Dis* 2017;59(1):369–85. Epub 2017/07/04. doi: 10.3233/JAD-170181. [PubMed: 28671118]

- Bennett RE, Robbins AB, Hu M, Cao X, Betensky RA, Clark T, Das S, Hyman BT. Tau induces blood vessel abnormalities and angiogenesis-related gene expression in P301L transgenic mice and human Alzheimer's disease. *Proc Natl Acad Sci U S A* 2018;115(6):E1289–E98. Epub 2018/01/24. doi: 10.1073/pnas.1710329115. [PubMed: 29358399]
- Besser L, Kukull W, Knopman DS, Chui H, Galasko D, Weintraub S, Jicha G, Carlsson C, Burns J, Quinn J, Sweet RA, Rascovsky K, Teylan M, Beekly D, Thomas G, Bollenbeck M, Monsell S, Mock C, Zhou XH, Thomas N, Robichaud E, Dean M, Hubbard J, Jacka M, Schwabe-Fry K, Wu J, Phelps C, Morris JC, Neuropsychology Work Group D, Clinical Core leaders of the National Institute on Aging-funded USAsDC. Version 3 of the National Alzheimer's Coordinating Center's Uniform Data Set. *Alzheimer Dis Assoc Disord* 2018;32(4):351–8. Epub 2018/10/31. doi: 10.1097/WAD.0000000000000279. [PubMed: 30376508]
- Binnewijzend MA, Kuijter JP, Benedictus MR, van der Flier WM, Wink AM, Wattjes MP, van Berckel BN, Scheltens P, Barkhof F. Cerebral blood flow measured with 3D pseudocontinuous arterial spin-labeling MR imaging in Alzheimer disease and mild cognitive impairment: a marker for disease severity. *Radiology* 2013;267(1):221–30. Epub 2012/12/15. doi: 10.1148/radiol.12120928. [PubMed: 23238159]
- Brett M, Anton J, Vlabregue R, Poline J. Region of interest analysis using an SPM toolbox [abstract] Presented at the 8th International Conference on Functional Mapping of the Human Brain, June 2–6, 2002, Sendai, Japan. Available on CD-ROM in NeuroImage, Vol 16, No 2, abstract 497.
- Butcher TJ, Chumin EJ, West JD, Dziedzic M, Yoder KK. Cerebral Blood Flow in the Salience Network of Individuals with Alcohol Use Disorder. *Alcohol Alcohol* 2021. Epub 2021/09/21. doi: 10.1093/alcac/agab062.
- Castellano JM, Kim J, Stewart FR, Jiang H, DeMattos RB, Patterson BW, Fagan AM, Morris JC, Mawuenyega KG, Cruchaga C, Goate AM, Bales KR, Paul SM, Bateman RJ, Holtzman DM. Human apoE isoforms differentially regulate brain amyloid-beta peptide clearance. *Sci Transl Med* 2011;3(89):89ra57. Epub 2011/07/01. doi: 10.1126/scitranslmed.3002156.
- Chan SL, Bishop N, Li Z, Cipolla MJ. Inhibition of PAI (Plasminogen Activator Inhibitor)-1 Improves Brain Collateral Perfusion and Injury After Acute Ischemic Stroke in Aged Hypertensive Rats. *Stroke* 2018;49(8):1969–76. Epub 2018/07/12. doi: 10.1161/STROKEAHA.118.022056. [PubMed: 29991657]
- Chen YJ, Rosario BL, Mowrey W, Laymon CM, Lu X, Lopez OL, Klunk WE, Lopresti BJ, Mathis CA, Price JC. Relative 11C-PiB Delivery as a Proxy of Relative CBF: Quantitative Evaluation Using Single-Session 15O-Water and 11C-PiB PET. *J Nucl Med* 2015;56(8):1199–205. Epub 2015/06/06. doi: 10.2967/jnumed.114.152405. [PubMed: 26045309]
- Codispoti KE, Beason-Held LL, Kraut MA, O'Brien RJ, Rudow G, Pletnikova O, Crain B, Troncoso JC, Resnick SM. Longitudinal brain activity changes in asymptomatic Alzheimer disease. *Brain Behav* 2012;2(3):221–30. Epub 2012/06/29. doi: 10.1002/brb3.47. [PubMed: 22741095]
- Congdon EE, Sigurdsson EM. Tau-targeting therapies for Alzheimer disease. *Nat Rev Neurol* 2018;14(7):399–415. Epub 2018/06/14. doi: 10.1038/s41582-018-0013-z. [PubMed: 29895964]
- Crous-Bou M, Minguillon C, Gramunt N, Molinuevo JL. Alzheimer's disease prevention: from risk factors to early intervention. *Alzheimers Res Ther* 2017;9(1):71. Epub 2017/09/14. doi: 10.1186/s13195-017-0297-z. [PubMed: 28899416]
- Dai W, Lopez OL, Carmichael OT, Becker JT, Kuller LH, Gach HM. Mild cognitive impairment and Alzheimer disease: patterns of altered cerebral blood flow at MR imaging. *Radiology* 2009;250(3):856–66. Epub 2009/01/24. doi: 10.1148/radiol.2503080751. [PubMed: 19164119]
- de la Torre JC, Pappas BA, Prevot V, Emmerling MR, Mantione K, Fortin T, Watson MD, Stefano GB. Hippocampal nitric oxide upregulation precedes memory loss and A beta 1–40 accumulation after chronic brain hypoperfusion in rats. *Neurol Res* 2003;25(6):635–41. Epub 2003/09/25. doi: 10.1179/016164103101201931. [PubMed: 14503018]
- Donahue JE, Johanson CE. Apolipoprotein E, amyloid-beta, and blood-brain barrier permeability in Alzheimer disease. *J Neuropathol Exp Neurol* 2008;67(4):261–70. Epub 2008/04/02. doi: 10.1097/NEN.0b013e31816a0dc8. [PubMed: 18379441]
- Faraco G, Park L, Zhou P, Luo W, Paul SM, Anrather J, Iadecola C. Hypertension enhances Aβ-induced neurovascular dysfunction, promotes β-secretase activity, and leads to amyloidogenic

- processing of APP. *J Cereb Blood Flow Metab* 2016;36(1):241–52. Epub 2015/04/30. doi: 10.1038/jcbfm.2015.79. [PubMed: 25920959]
- Fazlollahi A, Calamante F, Liang X, Bourgeat P, Raniga P, Dore V, Frripp J, Ames D, Masters CL, Rowe CC, Connelly A, Villemagne VL, Salvado O, Australian Imaging B, Lifestyle Research G. Increased cerebral blood flow with increased amyloid burden in the preclinical phase of alzheimer's disease. *J Magn Reson Imaging* 2020;51(2):505–13. Epub 2019/05/31. doi: 10.1002/jmri.26810. [PubMed: 31145515]
- Fischl B, Dale AM. Measuring the thickness of the human cerebral cortex from magnetic resonance images. *Proc Natl Acad Sci U S A* 2000;97(20):11050–5. Epub 2000/09/14. doi: 10.1073/pnas.200033797. [PubMed: 10984517]
- Gomez-Isla T, Hollister R, West H, Mui S, Growdon JH, Petersen RC, Parisi JE, Hyman BT. Neuronal loss correlates with but exceeds neurofibrillary tangles in Alzheimer's disease. *Ann Neurol* 1997;41(1):17–24. Epub 1997/01/01. doi: 10.1002/ana.410410106. [PubMed: 9005861]
- Gorelick PB. Risk factors for vascular dementia and Alzheimer disease. *Stroke* 2004;35(11 Suppl 1):2620–2. Epub 2004/09/18. doi: 10.1161/01.STR.0000143318.70292.47. [PubMed: 15375299]
- Hays CC, Zlatar ZZ, Meloy MJ, Osuna J, Liu TT, Galasko DR, Wierenga CE. Anterior Cingulate Structure and Perfusion is Associated with Cerebrospinal Fluid Tau among Cognitively Normal Older Adult APOEε4 Carriers. *J Alzheimers Dis* 2020;73(1):87–101. Epub 2019/11/21. doi: 10.3233/JAD-190504. [PubMed: 31743999]
- Iadecola C Neurovascular regulation in the normal brain and in Alzheimer's disease. *Nat Rev Neurosci* 2004;5(5):347–60. Epub 2004/04/22. doi: 10.1038/nrn1387. [PubMed: 15100718]
- Iadecola C, Gottesman RF. Neurovascular and Cognitive Dysfunction in Hypertension. *Circ Res* 2019;124(7):1025–44. Epub 2019/03/29. doi: 10.1161/CIRCRESAHA.118.313260. [PubMed: 30920929]
- Jack CR, Wiste HJ, Weigand SD, Therneau TM, Lowe VJ, Knopman DS, Botha H, Graff-Radford J, Jones DT, Ferman TJ, Boeve BF, Kantarci K, Vemuri P, Mielke MM, Whitwell J, Josephs K, Schwarz CG, Senjem ML, Gunter JL, Petersen RC. Predicting future rates of tau accumulation on PET. *Brain* 2020;143(10):3136–50. Epub 2020/10/24. doi: 10.1093/brain/awaa248. [PubMed: 33094327]
- Jagust WJ, Landau SM, Koeppe RA, Reiman EM, Chen K, Mathis CA, Price JC, Foster NL, Wang AY. The Alzheimer's Disease Neuroimaging Initiative 2 PET Core: 2015. *Alzheimers Dement* 2015;11(7):757–71. Epub 2015/07/22. doi: 10.1016/j.jalz.2015.05.001. [PubMed: 26194311]
- Jaworski T, Lechat B, Demedts D, Gielis L, Devijver H, Borghgraef P, Duimel H, Verheyen F, Kugler S, Van Leuven F. Dendritic degeneration, neurovascular defects, and inflammation precede neuronal loss in a mouse model for tau-mediated neurodegeneration. *Am J Pathol* 2011;179(4):2001–15. Epub 2011/08/16. doi: 10.1016/j.ajpath.2011.06.025. [PubMed: 21839061]
- Jessen F, Amariglio RE, van Boxtel M, Breteler M, Ceccaldi M, Chetelat G, Dubois B, Dufouil C, Ellis KA, van der Flier WM, Glodzik L, van Harten AC, de Leon MJ, McHugh P, Mielke MM, Molinuevo JL, Mosconi L, Osorio RS, Perrotin A, Petersen RC, Rabin LA, Rami L, Reisberg B, Rentz DM, Sachdev PS, de la Sayette V, Saykin AJ, Scheltens P, Shulman MB, Slavin MJ, Sperling RA, Stewart R, Uspenskaya O, Vellas B, Visser PJ, Wagner M, Subjective Cognitive Decline Initiative Working G. A conceptual framework for research on subjective cognitive decline in preclinical Alzheimer's disease. *Alzheimers Dement* 2014;10(6):844–52. Epub 2014/05/07. doi: 10.1016/j.jalz.2014.01.001. [PubMed: 24798886]
- Khan MB, Hoda MN, Vaibhav K, Giri S, Wang P, Waller JL, Ergul A, Dhandapani KM, Fagan SC, Hess DC. Remote ischemic postconditioning: harnessing endogenous protection in a murine model of vascular cognitive impairment. *Transl Stroke Res* 2015;6(1):69–77. Epub 2014/10/30. doi: 10.1007/s12975-014-0374-6. [PubMed: 25351177]
- Klohs J, Rudin M, Shimshek DR, Beckmann N. Imaging of cerebrovascular pathology in animal models of Alzheimer's disease. *Front Aging Neurosci* 2014;6:32. Epub 2014/03/25. doi: 10.3389/fnagi.2014.00032. [PubMed: 24659966]
- Lennon MJ, Koncz R, Sachdev PS. Hypertension and Alzheimer's disease: is the picture any clearer? *Curr Opin Psychiatry* 2021;34(2):142–8. Epub 2021/01/05. doi: 10.1097/YCO.0000000000000684. [PubMed: 33395097]

- Liang W, Zhang W, Zhao S, Li Q, Liang H, Ceng R. Altered expression of neurofilament 200 and amyloid-beta peptide (1–40) in a rat model of chronic cerebral hypoperfusion. *Neurol Sci* 2015;36(5):707–12. Epub 2014/12/03. doi: 10.1007/s10072-014-2014-z. [PubMed: 25452168]
- Lourenco CF, Ledo A, Barbosa RM, Laranjinha J. Neurovascular uncoupling in the triple transgenic model of Alzheimer's disease: Impaired cerebral blood flow response to neuronal-derived nitric oxide signaling. *Exp Neurol* 2017;291:36–43. Epub 2017/02/06. doi: 10.1016/j.expneurol.2017.01.013. [PubMed: 28161255]
- Lu L, Zheng X, Wang S, Tang C, Zhang Y, Yao G, Zeng J, Ge S, Wen H, Xu M, Guyatt G, Xu N. Anti-Abeta agents for mild to moderate Alzheimer's disease: systematic review and meta-analysis. *J Neurol Neurosurg Psychiatry* 2020;91(12):1316–24. Epub 2020/10/14. doi: 10.1136/jnnp-2020-323497. [PubMed: 33046560]
- Mahley RW, Weisgraber KH, Huang Y. Apolipoprotein E4: a causative factor and therapeutic target in neuropathology, including Alzheimer's disease. *Proc Natl Acad Sci U S A* 2006;103(15):5644–51. Epub 2006/03/29. doi: 10.1073/pnas.0600549103. [PubMed: 16567625]
- Mattsson N, Tosun D, Insel PS, Simonson A, Jack CR Jr., Beckett LA, Donohue M, Jagust W, Schuff N, Weiner MW, Alzheimer's Disease Neuroimaging I. Association of brain amyloid-beta with cerebral perfusion and structure in Alzheimer's disease and mild cognitive impairment. *Brain* 2014;137(Pt 5):1550–61. Epub 2014/03/15. doi: 10.1093/brain/awu043. [PubMed: 24625697]
- Michels L, Warnock G, Buck A, Macaudo G, Leh SE, Kaelin AM, Riese F, Meyer R, O'Gorman R, Hock C, Kollias S, Gietl AF. Arterial spin labeling imaging reveals widespread and Abeta-independent reductions in cerebral blood flow in elderly apolipoprotein epsilon-4 carriers. *J Cereb Blood Flow Metab* 2016;36(3):581–95. Epub 2015/12/15. doi: 10.1177/0271678X15605847. [PubMed: 26661143]
- Niwa K, Carlson GA, Iadecola C. Exogenous A beta1–40 reproduces cerebrovascular alterations resulting from amyloid precursor protein overexpression in mice. *J Cereb Blood Flow Metab* 2000;20(12):1659–68. Epub 2000/12/29. doi: 10.1097/00004647-200012000-00005. [PubMed: 11129782]
- Niwa K, Kazama K, Younkin L, Younkin SG, Carlson GA, Iadecola C. Cerebrovascular autoregulation is profoundly impaired in mice overexpressing amyloid precursor protein. *Am J Physiol Heart Circ Physiol* 2002;283(1):H315–23. Epub 2002/06/14. doi: 10.1152/ajpheart.00022.2002. [PubMed: 12063304]
- Niwa K, Porter VA, Kazama K, Cornfield D, Carlson GA, Iadecola C. A beta-peptides enhance vasoconstriction in cerebral circulation. *Am J Physiol Heart Circ Physiol* 2001;281(6):H2417–24. Epub 2001/11/16. doi: 10.1152/ajpheart.2001.281.6.H2417. [PubMed: 11709407]
- Nortley R, Korte N, Izquierdo P, Hirunpattarasilp C, Mishra A, Jaunmuktane Z, Kyrargyri V, Pfeiffer T, Khennouf L, Madry C, Gong H, Richard-Loendt A, Huang W, Saito T, Saido TC, Brandner S, Sethi H, Attwell D. Amyloid beta oligomers constrict human capillaries in Alzheimer's disease via signaling to pericytes. *Science* 2019;365(6450). Epub 2019/06/22. doi: 10.1126/science.aav9518.
- Ossenkoppele R, Schonhaut DR, Scholl M, Lockhart SN, Ayakta N, Baker SL, O'Neil JP, Janabi M, Lazaris A, Cantwell A, Vogel J, Santos M, Miller ZA, Bettcher BM, Vessel KA, Kramer JH, Gorno-Tempini ML, Miller BL, Jagust WJ, Rabinovici GD. Tau PET patterns mirror clinical and neuroanatomical variability in Alzheimer's disease. *Brain* 2016;139(Pt 5):1551–67. Epub 2016/03/11. doi: 10.1093/brain/aww027. [PubMed: 26962052]
- Park L, Hochrainer K, Hattori Y, Ahn SJ, Anfray A, Wang G, Uekawa K, Seo J, Palfini V, Blanco I, Acosta D, Eliezer D, Zhou P, Anrather J, Iadecola C. Tau induces PSD95-neuronal NOS uncoupling and neurovascular dysfunction independent of neurodegeneration. *Nat Neurosci* 2020;23(9):1079–89. Epub 2020/08/12. doi: 10.1038/s41593-020-0686-7. [PubMed: 32778793]
- Raz L, Bhaskar K, Weaver J, Marini S, Zhang Q, Thompson JF, Espinoza C, Iqbal S, Maphis NM, Weston L, Sillerud LO, Caprihan A, Pesko JC, Erhardt EB, Rosenberg GA. Hypoxia promotes tau hyperphosphorylation with associated neuropathology in vascular dysfunction. *Neurobiol Dis* 2019;126:124–36. Epub 2018/07/17. doi: 10.1016/j.nbd.2018.07.009. [PubMed: 30010004]
- Risacher SL, West JD, Deardorff R, Gao S, Farlow MR, Brosch JR, Apostolova LG, McAllister TW, Wu YC, Jagust WJ, Landau SM, Weiner MW, Saykin AJ, Alzheimer's Disease Neuroimaging I. Head injury is associated with tau deposition on PET in MCI and AD patients. *Alzheimers Dement (Amst)* 2021;13(1):e12230. Epub 2021/09/02. doi: 10.1002/dad2.12230. [PubMed: 34466653]

- Rodell AB, O'Keefe G, Rowe CC, Villemagne VL, Gjedde A. Cerebral Blood Flow and Abeta-Amyloid Estimates by WARM Analysis of [(11)C]PiB Uptake Distinguish among and between Neurodegenerative Disorders and Aging. *Front Aging Neurosci* 2016;8:321. Epub 2017/01/27. doi: 10.3389/fnagi.2016.00321. [PubMed: 28123366]
- Rubinski A, Tosun D, Franzmeier N, Neitzel J, Frontzkowski L, Weiner M, Ewers M. Lower cerebral perfusion is associated with tau-PET in the entorhinal cortex across the Alzheimer's continuum. *Neurobiol Aging* 2021;102:111–8. Epub 2021/03/26. doi: 10.1016/j.neurobiolaging.2021.02.003. [PubMed: 33765424]
- Saykin AJ, Wishart HA, Rabin LA, Santulli RB, Flashman LA, West JD, McHugh TL, Mamourian AC. Older adults with cognitive complaints show brain atrophy similar to that of amnesic MCI. *Neurology* 2006;67(5):834–42. Epub 2006/09/13. doi: 10.1212/01.wnl.0000234032.77541.a2. [PubMed: 16966547]
- Schwarz AJ, Yu P, Miller BB, Shcherbinin S, Dickson J, Navitsky M, Joshi AD, Devous MD Sr., Mintun MS. Regional profiles of the candidate tau PET ligand 18F-AV-1451 recapitulate key features of Braak histopathological stages. *Brain* 2016;139(Pt 5):1539–50. Epub 2016/03/05. doi: 10.1093/brain/aww023. [PubMed: 26936940]
- Stomrud E, Forsberg A, Hagerstrom D, Ryding E, Blennow K, Zetterberg H, Minthon L, Hansson O, Londos E. CSF biomarkers correlate with cerebral blood flow on SPECT in healthy elderly. *Dement Geriatr Cogn Disord* 2012;33(2–3):156–63. Epub 2012/06/23. doi: 10.1159/000338185. [PubMed: 22722670]
- Swinford CG, Risacher SL, Wu YC, Apostolova LG, Gao S, Bice PJ, Saykin AJ. Altered cerebral blood flow in older adults with Alzheimer's disease: a systematic review. *Brain Imaging Behav* 2023;17(2):223–256. Epub 2022/12/10. doi: 10.1007/s11682-022-00750-6. [PubMed: 36484922]
- Takahashi M, Tada T, Nakamura T, Koyama K, Momose T. Efficacy and Limitations of rCBF-SPECT in the Diagnosis of Alzheimer's Disease With Amyloid-PET. *Am J Alzheimers Dis Other Dement* 2019;34(5):314–21. Epub 2019/04/11. doi: 10.1177/1533317519841192. [PubMed: 30966759]
- Tosun D, Schuff N, Jagust W, Weiner MW, Alzheimer's Disease Neuroimaging I. Discriminative Power of Arterial Spin Labeling Magnetic Resonance Imaging and 18F-Fluorodeoxyglucose Positron Emission Tomography Changes for Amyloid-beta-Positive Subjects in the Alzheimer's Disease Continuum. *Neurodegener Dis* 2016;16(1–2):87–94. Epub 2015/11/13. doi: 10.1159/000439257. [PubMed: 26560336]
- van Dyck CH, Swanson CJ, Aisen P, Bateman RJ, Chen C, Gee M, Kanekiyo M, Li D, Reyderman L, Cohen S, Froelich L, Katayama S, Sabbagh M, Vellas B, Watson D, Dhadda S, Irizarry M, Kramer LD, Iwatsubo T. Lecanemab in Early Alzheimer's Disease. *N Engl J Med* 2023;388(1):9–21. Epub 2022/12/01. doi: 10.1056/NEJMoa2212948. [PubMed: 36449413]
- Visser D, Wolters EE, Verfaillie SCJ, Coomans EM, Timmers T, Tuncel H, Reimand J, Boellaard R, Windhorst AD, Scheltens P, van der Flier WM, Ossenkoppele R, van Berckel BNM. Tau pathology and relative cerebral blood flow are independently associated with cognition in Alzheimer's disease. *Eur J Nucl Med Mol Imaging* 2020;47(13):3165–75. Epub 2020/05/29. doi: 10.1007/s00259-020-04831-w. [PubMed: 32462397]
- Wahrle SE, Shah AR, Fagan AM, Smemo S, Kauwe JS, Grupe A, Hinrichs A, Mayo K, Jiang H, Thal LJ, Goate AM, Holtzman DM. Apolipoprotein E levels in cerebrospinal fluid and the effects of ABCA1 polymorphisms. *Mol Neurodegener* 2007;2:7. Epub 2007/04/14. doi: 10.1186/1750-1326-2-7. [PubMed: 17430597]
- Wang J, Alsop DC, Song HK, Maldjian JA, Tang K, Salvucci AE, Detre JA. Arterial transit time imaging with flow encoding arterial spin tagging (FEAST). *Magn Reson Med* 2003;50(3):599–607. Epub 2003/08/27. doi: 10.1002/mrm.10559. [PubMed: 12939768]
- Wang J, Peng G, Liu P, Tan X, Luo B, Alzheimer's Disease Neuroimaging I. Regulating effect of CBF on memory in cognitively normal older adults with different ApoE genotype: the Alzheimer's Disease Neuroimaging Initiative (ADNI). *Cogn Neurodyn* 2019;13(6):513–8. Epub 2019/11/20. doi: 10.1007/s11571-019-09536-x. [PubMed: 31741688]
- Whitmer RA, Sidney S, Selby J, Johnston SC, Yaffe K. Midlife cardiovascular risk factors and risk of dementia in late life. *Neurology* 2005;64(2):277–81. Epub 2005/01/26. doi: 10.1212/01.WNL.0000149519.47454.F2. [PubMed: 15668425]

- Wierenga CE, Hays CC, Zlatar ZZ. Cerebral blood flow measured by arterial spin labeling MRI as a preclinical marker of Alzheimer's disease. *J Alzheimers Dis* 2014;42 Suppl 4:S411–9. Epub 2014/08/28. doi: 10.3233/JAD-141467. [PubMed: 25159672]
- Wilson PW, D'Agostino RB, Levy D, Belanger AM, Silbershatz H, Kannel WB. Prediction of coronary heart disease using risk factor categories. *Circulation* 1998;97(18):1837–47. Epub 1998/05/29. doi: 10.1161/01.cir.97.18.1837. [PubMed: 9603539]
- Zhang ZH, Fang XB, Xi GM, Li WC, Ling HY, Qu P. Calcitonin gene-related peptide enhances CREB phosphorylation and attenuates tau protein phosphorylation in rat brain during focal cerebral ischemia/reperfusion. *Biomed Pharmacother* 2010;64(6):430–6. Epub 2010/06/12. doi: 10.1016/j.biopha.2009.06.009. [PubMed: 20537498]
- Zhang H, Wang Y, Lyu D, Li Y, Li W, Wang Q, Li Y, Qin Q, Wang X, Gong M, Jiao H, Liu W, Jia J. Cerebral blood flow in mild cognitive impairment and Alzheimer's disease: A systematic review and meta-analysis. *Ageing Res Rev* 2021;71:101450. Epub 2021/08/23. doi: 10.1016/j.arr.2021.101450. [PubMed: 34419673]
- Zlatar ZZ, Bischoff-Grethe A, Hays CC, Liu TT, Meloy MJ, Rissman RA, Bondi MW, Wierenga CE. Higher Brain Perfusion May Not Support Memory Functions in Cognitively Normal Carriers of the ApoE epsilon4 Allele Compared to Non-Carriers. *Front Aging Neurosci* 2016;8:151. Epub 2016/07/23. doi: 10.3389/fnagi.2016.00151. [PubMed: 27445794]

**Highlights**

- Lower medial temporal cerebral blood flow is associated with medial temporal tau
- Hypertension is associated with lower cerebral blood flow
- Hypertension affects the relationship between cerebral blood flow and amyloid

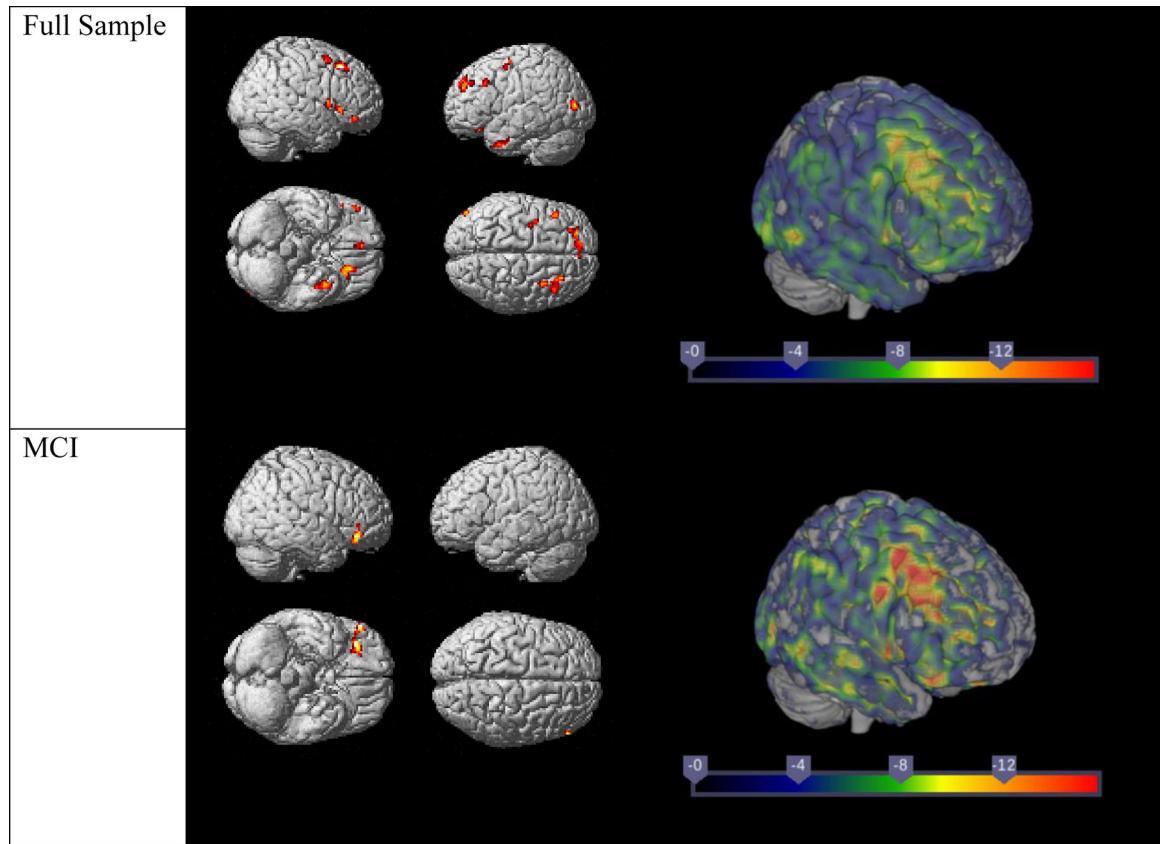


**Figure 1.** Negative correlations between voxel-wise CBF and self-reported hypertension status. Covariates are age, sex, diagnostic group and total gray matter volume. Images in left column illustrated at  $p < 0.001$ ;  $k = 50$ . Right column shows  $\beta$  maps.

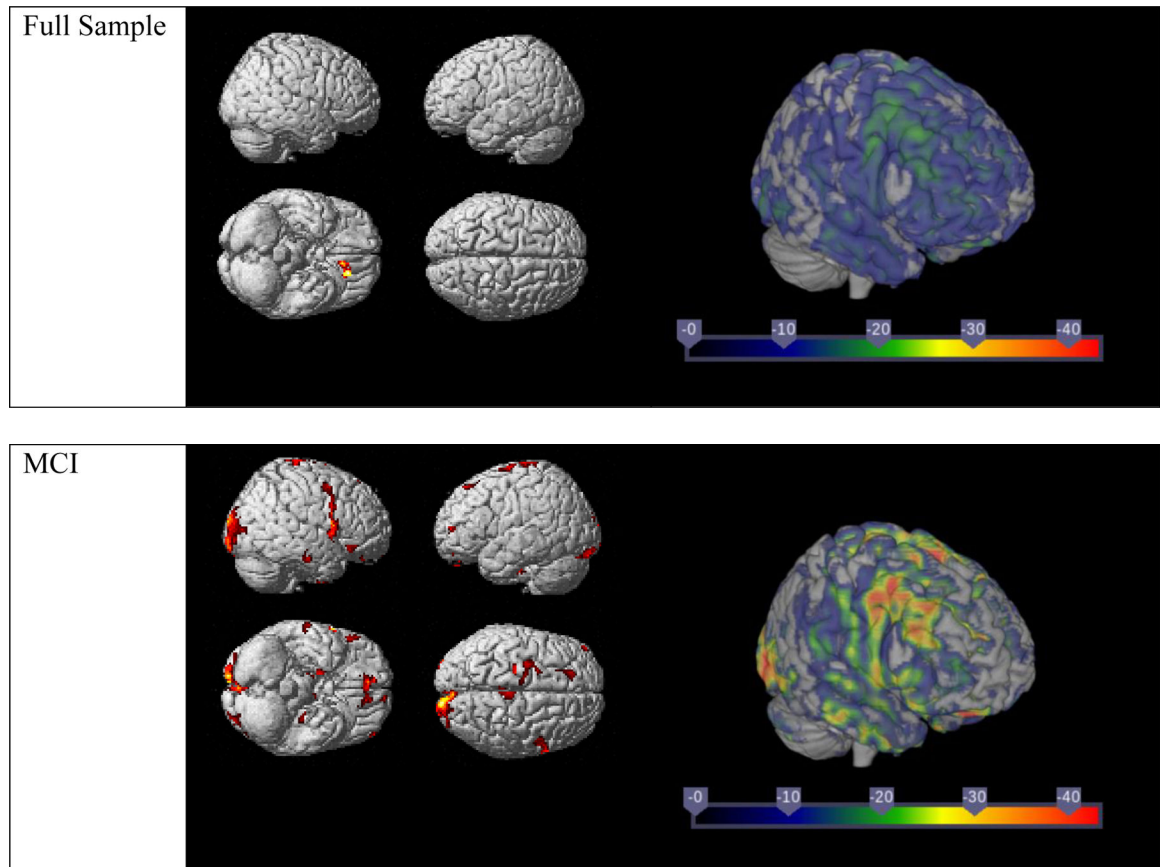


**Figure 2.** Negative correlations between voxel-wise CBF and self-reported hypertension status. Covariates are age, sex, diagnostic group, total gray matter volume vascular risk score and use of antihypertensive medication. Images in left column illustrated at  $p < 0.001$ ;  $k = 50$ . Right column shows  $\beta$  maps.

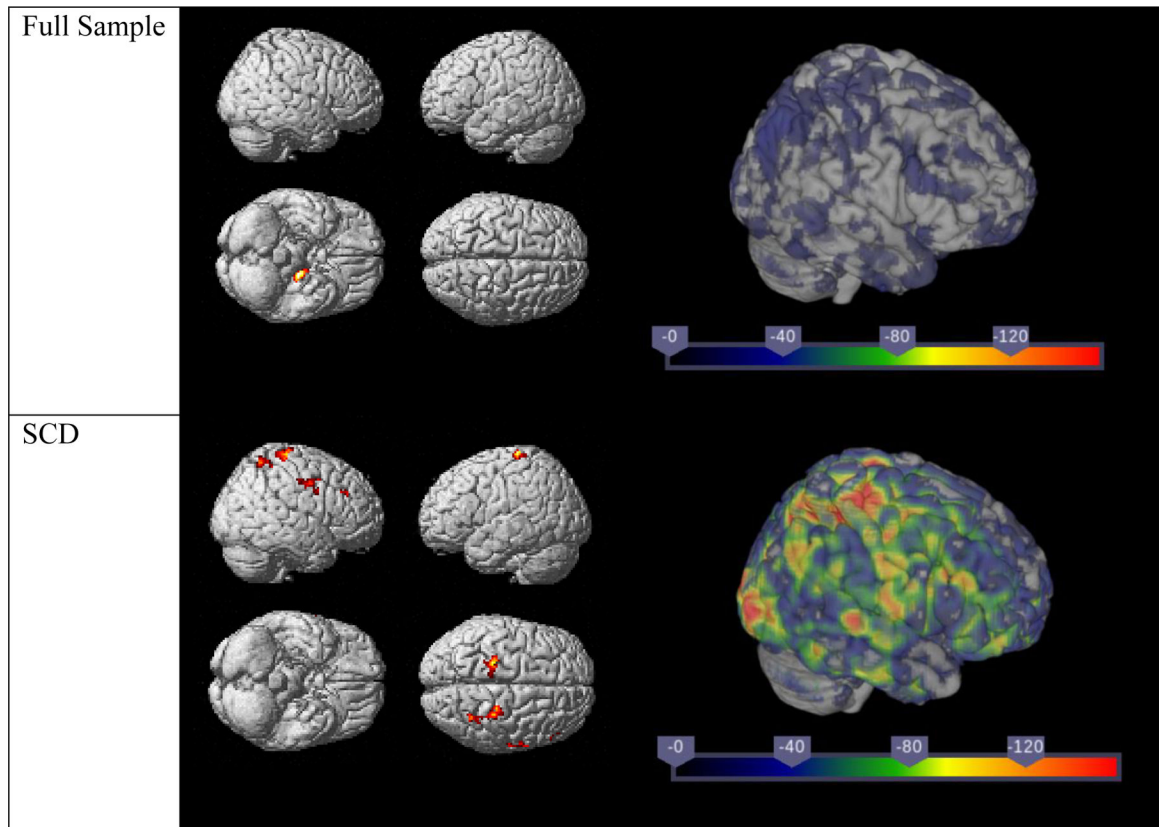


**Figure 3.** Negative correlations between voxel-wise CBF and MTL tau SUVR. Covariates are age, sex, diagnostic group, and total gray matter volume. Images in left column illustrated at  $p < 0.001$ ;  $k = 50$ . Right column shows  $\beta$  maps.

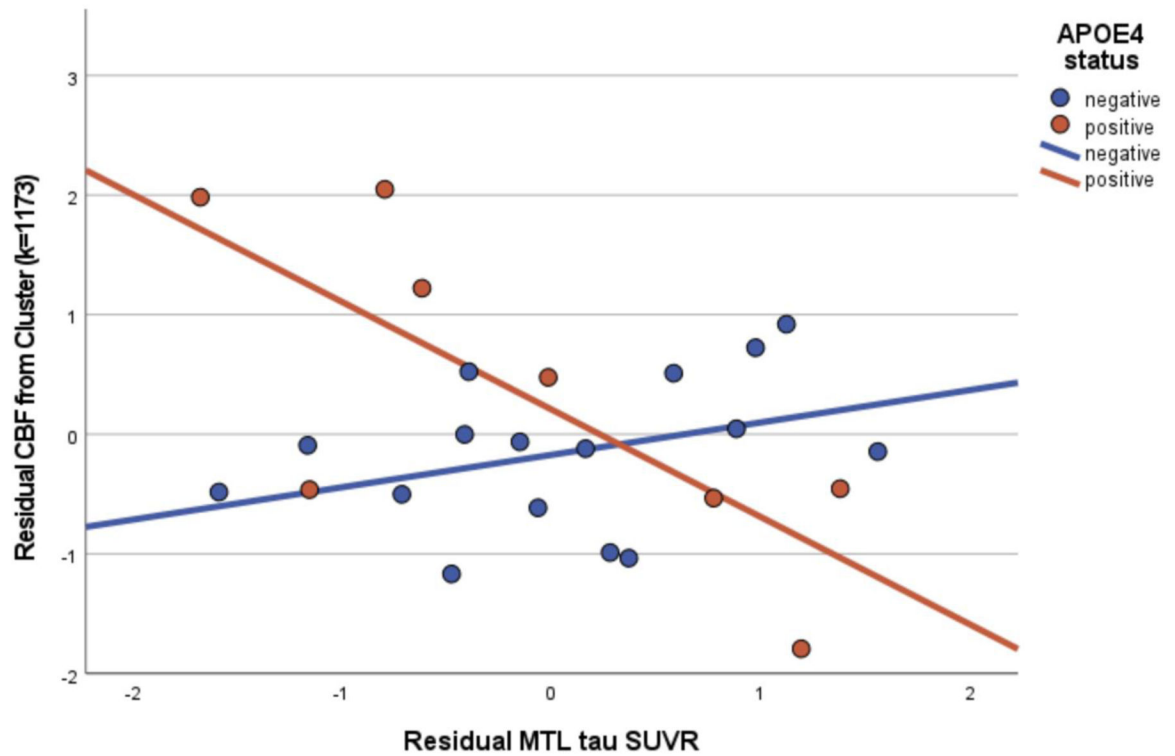


**Figure 4.** Scatterplot of the positive correlation between voxel-wise CBF and MTL tau SUVR in *APOE*  $\epsilon$ 4 negative individuals and the negative correlation between voxel-wise CBF and MTL tau SUVR in *APOE*  $\epsilon$ 4 positive individuals in the SCD group. Both the CBF and MTL tau SUVR plotted are standardized residuals from regressions with age, sex, and total gray matter volume. *APOE*  $\epsilon$ 4 negative  $R^2=0.137$ ,  $p=0.158$ ; *APOE*  $\epsilon$ 4 positive  $R^2=0.559$ ,  $p=0.033$ .

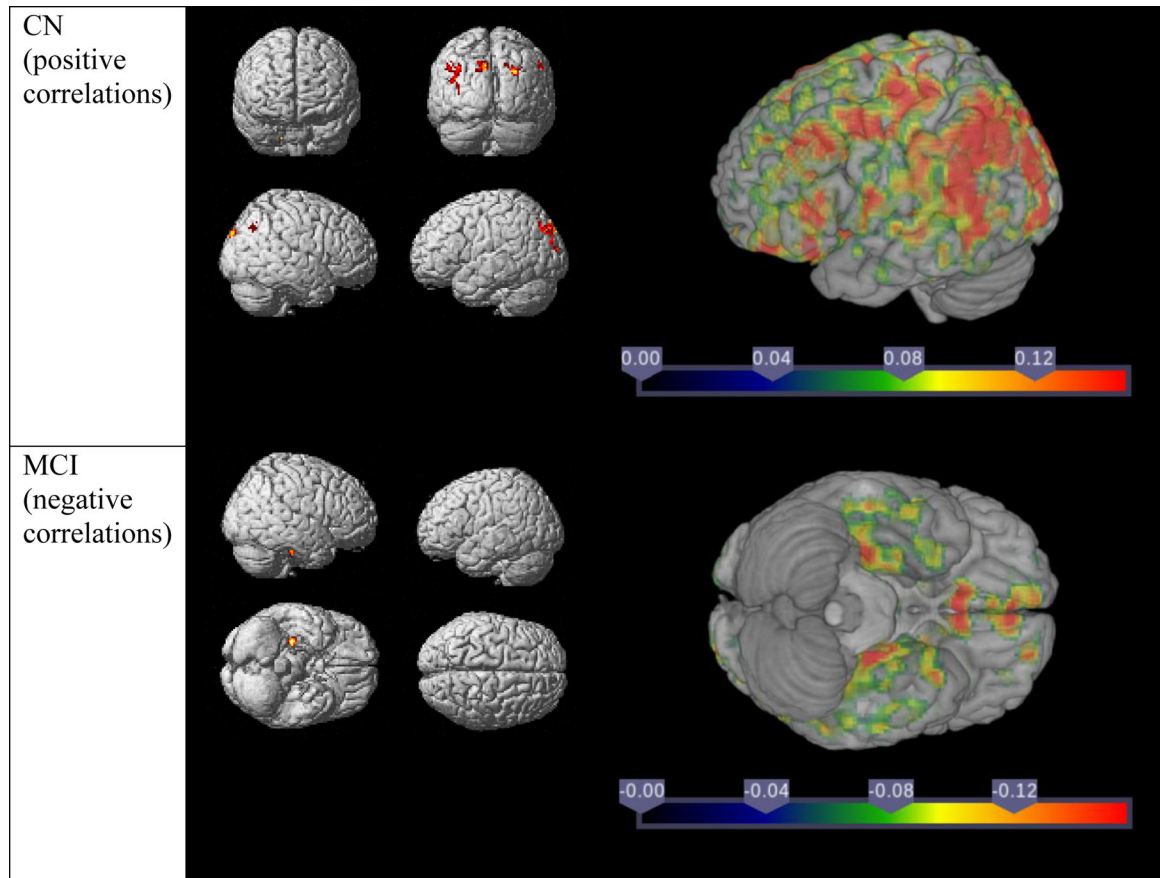


**Figure 5.** Correlations between voxel-wise CBF and global cortical Centiloid. Covariates are age, sex, and total gray matter volume. Images in left column illustrated at  $p$  0.001;  $k$  50. Right column shows  $\beta$  maps.

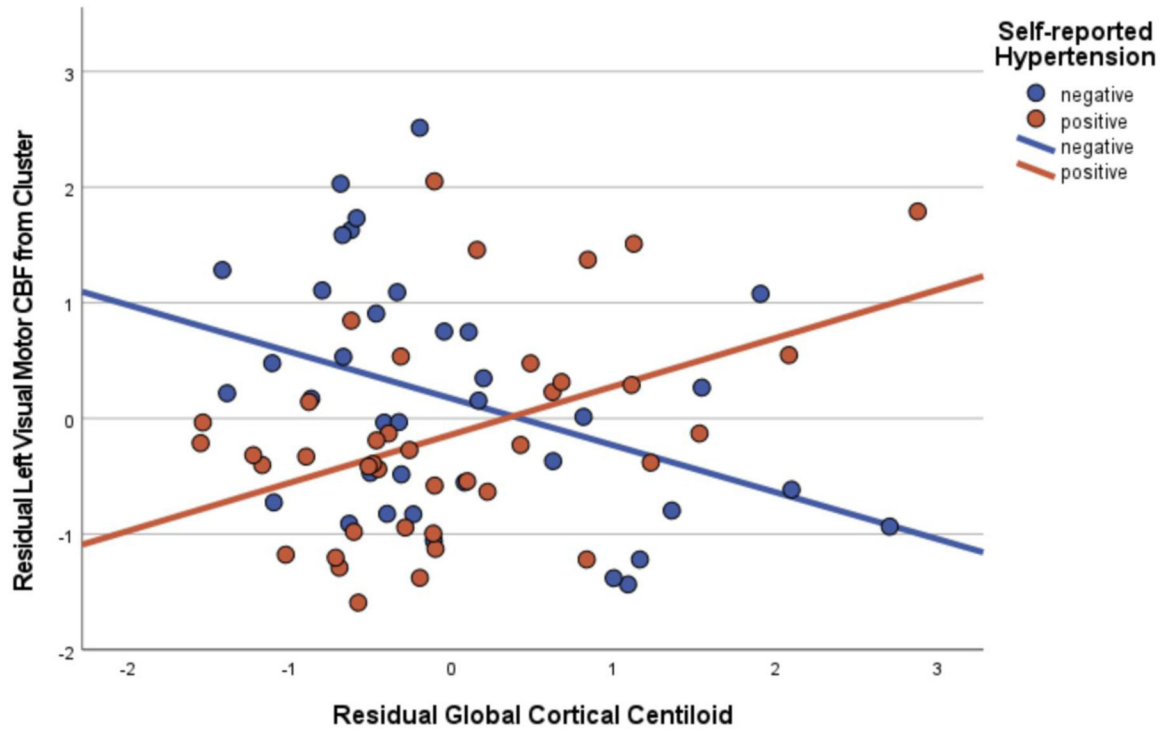


**Figure 6.**

Scatterplot of the negative correlation between voxel-wise CBF and global cortical Centiloid in individuals without self-reported hypertension (negative) and the positive correlation between voxel-wise CBF and global cortical Centiloid in individuals with self-reported hypertension (positive) in the whole sample. Both the CBF and global cortical Centiloid plotted are standardized residuals from regressions with age, sex, and total gray matter volume. Self-reported hypertension negative  $R^2=0.155$ ,  $p=0.016$ ; self-reported hypertension positive  $R^2=0.196$ ,  $p=0.004$ .

Table 1.

Demographic and clinical variables by diagnostic group.

|   | All (n=77)       | CN (n=30)        | SCD (n=24)       | MCI (n=23)       | Group Comparison <i>p</i> |
|---|------------------|------------------|------------------|------------------|---------------------------|
| Age   | 71.69 ± 6.75     | 71.03 ± 6.66     | 71.04 ± 6.88     | 73.22 ± 6.78     | 0.436                     |
| Sex (female)                                | 64.9% (50)       | 76.7% (23)       | 66.7% (16)       | 47.8% (11)       | 0.091                     |
| Education (years)                           | 16.44 ± 2.78     | 16.73 ± 2.55     | 16.54 ± 2.80     | 15.96 ± 3.11     | 0.595                     |
| Race (African American/Black)               | 14.3% (11)       | 16.7% (5)        | 20.8% (5)        | 4.3% (1)         | 0.242                     |
| Ethnicity (Hispanic)                        | 1.3% (1)         | 0% (0)           | 0% (0)           | 4.3% (1)         | 0.304                     |
| GM Volume (mm <sup>3</sup> )                | 571,221 ± 58,254 | 573,685 ± 58,882 | 574,368 ± 58,392 | 564,723 ± 59,372 | 0.819                     |
| Self-reported Hypertension                  | 51.9% (40)       | 30.0% (9)        | 75.0% (18)       | 56.5% (13)       | 0.004*<br>SCD > MCI > CN  |
| Global CBF (mL/100g/min)                    | 24.15 ± 6.28     | 24.66 ± 7.86     | 24.03 ± 5.24     | 23.62 ± 5.04     | 0.836                     |
| APOE ε4 positive                            | 42.9% (33)       | 43.3% (13)       | 33.3% (8)        | 52.2% (12)       | 0.426                     |
| Amyloid (Aβ) PET (Centiloid)                | 19.79 ± 32.17    | 10.31 ± 24.43    | 12.70 ± 26.74    | 39.54 ± 38.16    | 0.001*<br>MCI > CN&SCD    |
| Aβ positive (global cortical Centiloid >21) | 32.5% (25)       | 20.0% (6)        | 25.0% (6)        | 56.5% (13)       | 0.012*                    |
| Tau PET (SUVR)                              | 1.11 ± 0.11      | 1.10 ± 0.09      | 1.09 ± 0.06      | 1.15 ± 0.16      | 0.174                     |
| Vascular Risk Score                         | 1.78 ± 1.02      | 1.60 ± 1.13      | 1.87 ± 1.12      | 1.91 ± 0.73      | 0.471                     |
| Systolic BP                                 | 134.31 ± 19.00   | 134.53 ± 21.56   | 130.75 ± 13.51   | 137.74 ± 20.41   | 0.456                     |
| Diastolic BP                                | 71.73 ± 9.46     | 72.00 ± 9.23     | 71.46 ± 10.67    | 71.65 ± 8.81     | 0.978                     |
| Hypertension                                | 61.0% (47)       | 60.0% (18)       | 58.3% (14)       | 65.2% (15)       | 0.880                     |
| BMI   | 28.25 ± 5.26     | 27.61 ± 5.36     | 29.15 ± 5.87     | 28.15 ± 4.50     | 0.568                     |
| Self-reported Diabetes                      | 18.2% (14)       | 10.0% (3)        | 29.2% (7)        | 17.3% (4)        | 0.191                     |
| Self-reported Hypercholesterolemia          | 66.2% (51)       | 60.0% (18)       | 62.5% (15)       | 78.3% (18)       | 0.340                     |
| Hypertension Medication                     | 53.2% (41)       | 36.7% (11)       | 66.7% (16)       | 60.9% (14)       | 0.061 <sup>^</sup>        |
| Hypercholesterolemia Medication             | 54.5% (42)       | 53.3% (16)       | 45.8% (11)       | 65.2% (15)       | 0.405                     |
| Diabetes Medication                         | 15.6% (12)       | 13.3% (4)        | 25.0% (6)        | 8.7% (2)         | 0.278                     |

APOE: apolipoprotein E, BMI: body mass index, BP: blood pressure, CBF: cerebral blood flow, CN: cognitively normal, GM: gray matter, MCI: mild cognitive impairment, PET: positron emission tomography, SCD: subjective cognitive decline, SUVR: standardized uptake value ratio;

\*  $p < 0.05$

<sup>^</sup>  $0.05 < p < 0.075$

**Table 2.**

Correlation of age, self-reported hypertension status, and female sex with lobar CBF.

|           | Independent Variable retained in Model | Standardized Coefficient ( $\beta$ ) | <i>t</i> | <i>p</i> |
|-----------|--|--------------------------------------|----------|----------|
| Frontal   | Age                                    | -0.343                               | -3.362   | 0.001    |
|           | Self-reported Hypertension             | -0.315                               | -3.095   | 0.003    |
|           |  |                                      |          |          |
| Limbic    | Age                                    | -0.307                               | -2.947   | 0.004    |
|           | Self-reported Hypertension             | -0.210                               | -2.009   | 0.048    |
|           | Sex                                    | 0.219                                | 2.104    | 0.039    |
| Parietal  | Age                                    | -0.307                               | -2.901   | 0.005    |
|           | Self-reported Hypertension             | -0.262                               | -2.478   | 0.015    |
|           |  |                                      |          |          |
| Temporal  | Age                                    | -0.334                               | -3.194   | 0.002    |
|           | Self-reported Hypertension             | -0.267                               | -2.555   | 0.013    |
|           |  |                                      |          |          |
| Occipital | Age                                    | -0.298                               | -2.924   | 0.005    |
|           | Self-reported Hypertension             | -0.216                               | -2.114   | 0.038    |
|           |  |                                      |          |          |
|           | Sex                                    | 0.278                                | 2.724    | 0.008    |

Author Manuscript

Author Manuscript

Author Manuscript

Author Manuscript